

15. Scanlan, R. H. *Introduction to the Study of Aircraft Vibration and Flutter* (McMillan, New York, 1951).
16. Paidoussis, M. P. *Fluid–Structure Interaction* Vol. I (Academic, San Diego, 1998).
17. Fitt, A. D. & Pope, M. P. The unsteady motion of a two-dimensional flag with bending stiffness. *J. Eng. Sci.* (submitted).
18. Chomaz, J. M. & Cathalau, B. Soap films as two-dimensional classical fluids. *Phys. Rev. A* **41**, 2243–2245 (1990).
19. Lopez-Ruiz, R. & Pomeau, Y. Transition between two oscillation modes. *Phys. Rev. E* **55**, R3820–R3823 (1997).
20. Peschard, I. & Le Gal, P. Coupled wakes of cylinders. *Phys. Rev. Lett.* **77**, 3122–3125 (1996).
21. Peschard, I., Le Gal, P. & Takeda, Y. On the spatio-temporal structure of cylinder wakes. *Exp. Fluids* **26**, 188–196 (1999).

**Acknowledgements**

We thank L. Becker, A. Belmonte, F. Hayot and C. Wiggins for helpful discussions. We thank D. Havir for assistance with the LDV measurements. This work was supported in part by the National Science Foundation and by the Department of Energy.

Correspondence and requests for materials should be addressed to J.Z. (e-mail: jun@cims.nyu.edu).

**Observation of five-fold local symmetry in liquid lead**

H. Reichert\*, O. Klein\*†, H. Dosch\*, M. Denk\*, V. Honkimäki‡, T. Lippmann§ & G. Reiter||

\* Max-Planck-Institut für Metallforschung, 70569 Stuttgart, Germany  
 ‡ European Synchrotron Radiation Facility ESRF, 38043 Grenoble, France  
 § Hamburger Synchrotronstrahlungslabor HASYLAB, 22607 Hamburg, Germany  
 || Physics Department, University of Houston, Houston, Texas 77204-5506, USA

The local point symmetry of the short-range order in simple monatomic liquids remains a fundamental open question in condensed-matter science. For more than 40 years it has been conjectured<sup>1–4</sup> that liquids with centrosymmetric interactions may be composed of icosahedral building blocks. But these proposed mobile, randomly orientated structures have remained experimentally inaccessible owing to the unavoidable averaging involved in scattering experiments, which can therefore determine only the isotropic radial distribution function. Here we overcome this limitation by capturing liquid fragments at a solid–liquid interface, and observing the scattering of totally internally reflected (evanescent) X-rays, which are sensitive only to the liquid structure at the interface. Using this method, we observe five-fold local symmetry in liquid lead adjacent to a silicon wall, and obtain an experimental portrait of the icosahedral fragments that are predicted to occur in all close-packed monatomic liquids. By shedding new light on local bond order in disordered structures such as liquids and glasses, these results should lead to a better microscopic understanding of melting, freezing and supercooling.

The crystalline solid state is characterized by a long-range positional order of the atomic density at position  $\mathbf{r}$ ,  $\rho_s(\mathbf{r}) = \sum_m \delta(\mathbf{r} - \mathbf{R}_m)$ , where  $\mathbf{R}_m$  denotes the lattice positions of the atoms, and an associated orientational bond order belonging to one of the well-known allowed one-, two-, three-, four- or six-fold crystalline symmetries. In a diffraction experiment,  $\delta$ -function Bragg reflections

$$S_s(\mathbf{q}) = \int \rho_s(\mathbf{r}) e^{i\mathbf{q}\cdot\mathbf{r}} d\mathbf{r} = \sum_{HKL} \delta(\mathbf{q} - \mathbf{G}_{HKL}) \quad (1)$$

that is, ‘Laue spots’, are observed that show the associated point symmetry of the lattice. Here  $\mathbf{q} = \mathbf{k}_f - \mathbf{k}_i$  is the momentum transfer

given by the incident and diffracted wavevectors  $\mathbf{k}_i$  and  $\mathbf{k}_f$ , respectively, and  $\mathbf{G}_{HKL}$  are the reciprocal lattice vectors). In contrast, the liquid state exhibits short-range order extending only a few atomic distances given by the liquid correlation length  $\xi$ , which is typically in the range 3–8 Å in simple liquids. It can in principle be determined from the associated liquid pair correlation function  $g_l(r)$ . Even simple liquids can be considerably supercooled<sup>5</sup>, indicating a pronounced barrier to the transition between the supercooled metastable liquid and the thermodynamically stable solid. This supercooling phenomenon may be understood by assuming that the local liquid correlations have non-crystalline symmetries that have to be broken in the crystallization process. In fact, since the early work by Frank<sup>1</sup>, Bernal<sup>2,4</sup> and Scott<sup>3</sup>, a number of authors have proposed that the local liquid correlations in monatomic liquids, which exhibit centrosymmetric interactions favouring a close-packed local environment, are composed of defective or fragmented icosahedral building blocks that exhibit a five-fold symmetry<sup>1–4,6–8</sup> (Fig. 1a). As these local liquid correlations are isotropically distributed, a conventional diffraction experiment unavoidably yields a 4 $\pi$  average:

$$S_l(q) = 1 + \rho_o \int [g_l(r) - 1] e^{i\mathbf{q}\cdot\mathbf{r}} d\mathbf{r} \quad (2)$$

this permits access only to the pair correlation function  $g_l(r)$  of the liquid. Consequently, the intrinsic local liquid symmetry has withstood any experimental access. For a scattering experiment attempting to reveal the local liquid symmetry, a microscopic mechanism has to be provided that is able to capture the liquid building blocks in space and time. Here we show that this can in fact be achieved at solid–liquid interfaces by an appropriate combination of solid and liquid components.

At solid–liquid interfaces, the crystalline potential acts on the adjacent liquid in two ways. (1) Perpendicular to the wall, a liquid density oscillation appears within an interfacial layer of thickness  $\xi^*$  (see ref. 9 for a review). This hard-wall-induced packing effect has been observed at various solid–liquid interfaces<sup>10–12</sup> as well as at free metallic liquid surfaces<sup>13,14</sup>. (2) In the lateral direction  $\mathbf{r}_\parallel$ , the

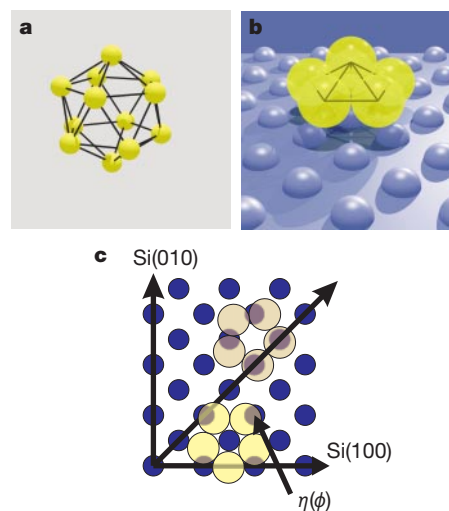


**Figure 1** View of the dominant motif in the structure of bulk liquid lead and of interfacial liquid lead. **a**, Polytetrahedral arrangement predicted for close-packed monatomic liquids. **b**, Upper (pentagonal) half of the Pb icosahedron (**a**) captured by the potential landscape of the primitive Si(001) surface. **c**, Projection of the pentagonal structure onto four-fold coordinated sites of the Si(001) surface (lower pentagon, upper site position with minimum overlap of the projected electron density for rotation angle  $\phi_n = 2\pi n/20$ , where  $n$  is an integer; upper pentagon, hollow site with minimum overlap for  $\phi_n = 2\pi(n+1/2)/20$ ; the overlap is denoted by  $\eta$  and shown in Fig. 3c as a function of the rotation  $\phi$  of the pentagon).

† Deceased.

periodic wall potential  $V(\mathbf{r}_\parallel) = \sum_{HK} V_{HK} \exp(iq_{HK}\mathbf{r}_\parallel)$  imposes its periodicity, as reflected in the coefficients  $V_{HK}$  (ref. 15), onto the ‘contact-liquid’, where  $H, K$  are conventional Miller indices.

Various theories have considered the case of a Lennard–Jones liquid that wets its own solid phase<sup>16–18</sup>. Here we consider a situation in which the wall and the liquid consist of incompatible materials: a monatomic liquid metal in contact with a solid semiconductor. In this case, the wall exhibits only a small lateral periodic perturbation potential  $V(\mathbf{r}_\parallel)$ , which is incommensurate with the liquid nearest-neighbour distances. Consequently, there is no wall-induced long-range translational ordering. On the other hand, the substrate potential may still be strong enough to capture a fraction of the predicted bulk liquid building blocks in preferred orientations, giving rise to orientational alignment. A properly designed X-ray scattering experiment from these aligned liquid fragments should then allow access to their local symmetry. For the experiment described below, we have chosen the incommensurate combination of liquid lead—which exhibits close-packed face-centred-cubic, f.c.c., structure (lattice constant  $a_{\text{Pb}} = 4.95 \text{ \AA}$  in the solid state)—in contact with Si(001), which has a diamond lattice with  $a_{\text{Si}} = 5.43 \text{ \AA}$ .

To date, no experimental information regarding the lateral microscopic structure of a liquid in contact with a wall has been available. This is due to the difficulties of designing a scattering experiment that is sensitive only to the liquid structure at the interface. It can, in principle, be achieved by exploiting total internal reflection of X-rays (Fig. 2a). In this scheme, a high-energy X-ray microbeam illuminates the interface from the solid side and is totally reflected. By this experimental device, non-propagating (evanescent) X-rays are created within the liquid adjacent to the wall while the X-ray field is absent in the bulk liquid. The in-plane liquid scattering from this evanescent X-ray field thus gives direct

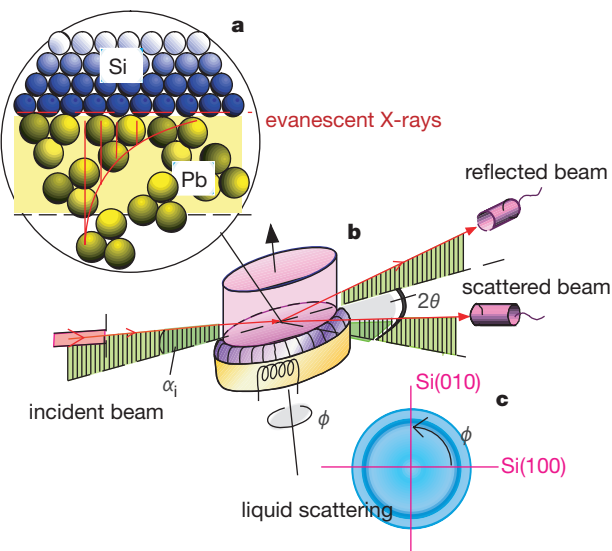


**Figure 2** Schematic set-up of the diffraction experiment. **a**, A well defined synchrotron high-energy X-ray microbeam ( $E = 71.5 \text{ keV}$ ,  $8 \mu\text{m}$  size) penetrates the cylindrical Si solid ( $r = 20 \text{ mm}$ ) from the side, and impinges at grazing angles on the Pb–Si interface. For incidence angles below the critical angle of total internal reflection ( $\alpha_c = 0.041^\circ$ ) the incident beam is totally reflected. The angle of incidence  $\alpha_i$  and the position of the interface in the X-ray beam are controlled to an accuracy of  $4 \mu\text{rad}$  and  $0.1 \mu\text{m}$ . This allows the exclusion of any bulk liquid scattering contributions from the edges of the interface. **b**, In a specially designed ultrahigh vacuum (UHV) *in situ* diffraction chamber, the liquid Pb and the Si(001) surface are cleaned in UHV and then brought into contact at a temperature 10 K greater than the melting point of lead. A  $360^\circ$  Be window allows free access of the beam to the solid–liquid interface. **c**, Top view of the in-plane rotation  $\phi$  at fixed momentum transfer  $q$  on the liquid scattering ring.

access to the local liquid structure in contact with the wall. Such experiments are now just feasible at third-generation synchrotron sources. Figure 2b shows schematically such a synchrotron X-ray scattering experiment, as realized at the high-energy X-ray diffraction stations ID15A and BW5 of the European Synchrotron Radiation Facility (ESRF) and of the Hamburg Synchrotron Radiation Laboratory (HASYLAB), respectively<sup>19,20</sup>.

We used two scattering schemes. (1) By using an in-plane detector scan ( $2\theta$  scan, see Fig. 2b), we have measured the liquid structure factor parallel to the wall. A typical experimental result is shown in Fig. 3a, disclosing a scattering intensity distribution that is characteristic of bulk-like liquid correlations; this implies that the bulk liquid structure of Pb (ref. 21) is essentially preserved in the contact regime (see also ref. 22). In particular, the position of the first structure factor maximum,  $q_1 = 2.18 \text{ \AA}^{-1}$ , agrees with the known bulk value. (2) By maintaining the  $2\theta$  angle around the first diffraction maximum (see marked positions in Fig. 3a), azimuthal scans ( $\phi$  scan, see Fig. 2b, c) were performed. In a bulk liquid, this type of scan inevitably shows a constant intensity associated with the random orientation of the liquid fragments. However, if the solid periodic potential is able to align preferred

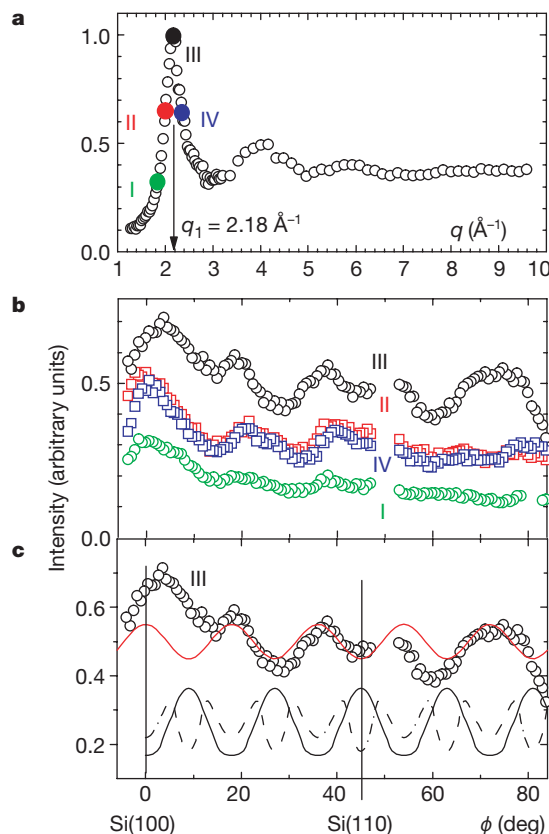


**Figure 3** Scattering at the interface between liquid lead and Si(001). **a**, Structure factor of liquid Pb ( $2\theta$  scan) measured in arbitrary units at an incidence angle  $\alpha_i = 0.032^\circ$  well below the critical angle for total internal reflection. The evanescent X-ray wave ‘tunnels’  $55 \text{ \AA}$  deep into the liquid Pb (see Fig. 2a). The background scattering from the Si substrate has been measured and subtracted. The values of momentum transfer (I–IV) at which the in-plane anisotropy of the liquid structure factor has been tested experimentally are marked on the curve. **b**, Azimuthal distribution of the liquid scattering at the four fixed momentum transfer values ( $\phi$  scans) marked in **a**. **c**, Azimuthal distribution of the liquid scattering in the first diffraction maximum. The red line is a fit of a sine wave to the experimental data in curve III (circles). The two lower lines show the total electron density overlap (see main text) of the pentagons with the underlying Si substrate versus pentagon rotation for the upper site position (full curve) and the hollow site position (dashed dotted curve). The epitaxial relation to the Si substrate is indicated by vertical lines.

orientations of the liquid building blocks, it should be possible to observe the characteristic intensity modulations from the local symmetry of these fragments. Our experimental observations for a  $\phi$  scan within a  $90^\circ$  segment of the non-reconstructed four-fold Si(001) wall is shown in Fig. 3b: a pronounced modulation of the liquid scattering intensity is found. We observe five intensity maxima with a fixed epitaxial relationship to the substrate (Fig. 3b). We find this modulation only for momentum transfer values close to the maximum of the liquid structure factor (curves II–IV).

The non-crystalline symmetry of this intensity modulation can only be understood as a convolution of a four-fold and a five-fold symmetry, whereby the four-fold symmetry is clearly imposed by the Si(001) substrate and the orientational part of the associated Si–Pb interface interaction  $V_o^{(Pb-Si)}$ . This remains the only relevant interaction when Pb is adsorbed on Si(001) in the submonolayer regime. A similar situation has been investigated in detail by surface-sensitive X-ray diffraction at the Pb–Ge(111) interface<sup>23</sup>, disclosing a substrate-modulated two-dimensional Pb liquid governed by the substrate symmetry only. This implies that the five-fold symmetry observed in our study emerges when bulk liquid Pb is brought in contact with the Si wall; that is, when the additional bulk Pb–Pb interaction  $V_o^{(Pb-Pb)}$  is introduced. The observed bulk-like in-plane liquid structure (Fig. 3a) gives unambiguous evidence that  $V_o^{(Pb-Pb)}$  is now dominating, while  $V_o^{(Pb-Si)}$  is a two-dimensional perturbation leading to a preferred alignment of a certain fraction  $n_{align}(z)$  of the liquid building blocks.

The observed relative intensity modulation  $\Delta I_{mod}/I$  in Fig. 3b, c is directly related to  $n_{align}(z)$ . To quantify this, if we denote  $\xi_{pb}$  as the correlation length within liquid Pb,  $\xi_{pb} = 5\text{--}8\text{ \AA}$ , then the depth-dependent alignment potential is given by

$$V_o^{(Pb-Si)}(z) = V_o^{(Pb-Si)} e^{-z/\xi_{pb}} \quad (3)$$

and in turn:

$$n_{align}(z) = 1 - e^{-V_o^{(Pb-Si)}(z)/k_B T} \quad (4)$$

As the evanescent X-rays decay exponentially with depth within  $\Lambda = 55\text{ \AA}$ ,  $\Delta I_{mod}/I$  and  $n_{align}(z)$  are related by<sup>24</sup>:

$$\frac{\Delta I_{mod}}{I} = \frac{1}{\Lambda} \int_0^\infty n_{align}(z) e^{-z/\Lambda} dz \quad (5)$$

Inserting equations (3) and (4) into equation (5), and using the experimentally determined value  $\Delta I_{mod}/I = 0.10 \pm 0.05$  (from Fig. 3c), the value of  $V_o^{(Pb-Si)}$  can be estimated numerically. This is shown in Fig. 4, which gives  $V_o^{(Pb-Si)} = 50\text{--}90\text{ meV}$  for the orientational part of the interface potential, depending on the detailed assumption of the interface-related value of  $\xi_{pb}$  (which may be

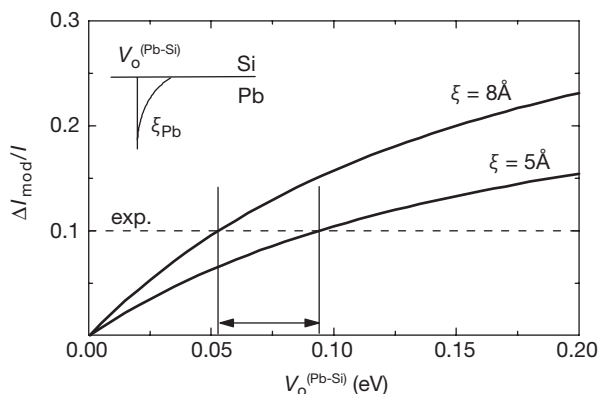


**Figure 4** Determination of the Si–Pb interface potential from the amplitude of the azimuthal relative intensity modulation  $\Delta I_{mod}/I$ . Assuming a range of  $5\text{--}8\text{ \AA}$  for the specific value of the bulk correlation length  $\xi_{pb}$  (see inset) we obtain a range of  $50\text{--}90\text{ meV}$  for the interface potential.

slightly different from the bulk value). Thus, the observed value of the modulation amplitude is directly correlated with a thermal interface energy, and comparable to  $kT_m \approx 50\text{ meV}$  at the melting temperature ( $T_m$ ) of lead,  $600.6\text{ K}$ . The value of the bulk binding energy  $V_o^{(Pb-Pb)}$ , on the other hand, is given by the cohesive energy  $V_o^{(Pb-Pb)} = 2.0\text{ eV}$ , implying that  $V_o^{(Pb-Si)}/V_o^{(Pb-Pb)} \approx 10^{-2}$ .

Figure 1b shows such liquid building blocks (the upper fragment of the icosahedron of Fig. 1a) attached to the Si(001) surface such that one Si surface atom is located at the centre of a pentagon of Pb atoms, thereby giving rise to the four-fold symmetric repetition of the five-fold modulation. The energetically favourable in-plane orientations of these pentagons are then found by determining those orientations (see Fig. 1c) where the projected electron density of the pentagonal building blocks has the minimum overlap ( $\eta$  in Fig. 1c) with the underlying Si atoms. This geometric argument predicts the maxima of the measured azimuthal intensity distribution at the experimentally observed positions (see Fig. 3c). The overlap varies over the underlying Si atoms, and this qualitatively accounts for the breadth of the five-fold oscillations. Also shown (in Fig. 1c) is a simulation for Pb pentagons centred at the other available four-fold coordinated site on the primitive Si(001) surface, the hollow site (Fig. 1c). This adsorption site is excluded unambiguously by our data.  $\square$

Received 13 July; accepted 16 October 2000.

- Frank, F. C. Supercooling of liquids. *Proc. R. Soc. Lond. A* **215**, 43–46 (1952).
- Bernal, J. D. Geometry of the structure of monatomic liquids. *Nature* **185**, 68–70 (1960).
- Scott, G. D. Radial distribution of the random close packing of equal spheres. *Nature* **194**, 956–957 (1962).
- Bernal, J. D. The structure of liquids. *Proc. R. Soc. Lond. A* **280**, 299–322 (1964).
- Turnbull, D. Kinetics of solidification of supercooled liquid mercury droplets. *J. Chem. Phys.* **20**, 411–424 (1952).
- Finney, J. L. Random packings and the structure of simple liquids. *Proc. R. Soc. Lond. A* **319**, 497–493; 495–507 (1970).
- Steinhardt, P. J., Nelson, D. R. & Ronchetti, M. Bond-orientational order in liquids and glasses. *Phys. Rev. B* **28**, 784–805 (1983).
- Nelson, D. R. & Spaepen, F. Polytetrahedral order in condensed matter. *Solid State Phys.* **42**, 1–90 (1989).
- Ocko, B. (ed.) *Focus on Liquid Interfaces* (Vol. 12, Synchrotron Radiation News, Gordon & Breach, Newark, 1999).
- Tooney, M. F. *et al.* Voltage-dependent ordering of water molecules at an electrode-electrolyte interface. *Nature* **368**, 444–446 (1994).
- Huisman, W. J. *et al.* Layering of a liquid metal in contact with a hard wall. *Nature* **390**, 379–381 (1997).
- Yu, C.-J., Richter, A. G., Datta, A., Durbin, M. K. & Dutta, P. Observation of molecular layering in thin liquid films using x-ray reflectivity. *Phys. Rev. Lett.* **82**, 2326–2329 (1999).
- Magnussen, O. M. *et al.* X-ray reflectivity measurements of surface layering in liquid mercury. *Phys. Rev. Lett.* **74**, 4444–4447 (1995).
- Regan, M. J. *et al.* Surface layering in liquid gallium: an x-ray reflectivity study. *Phys. Rev. Lett.* **75**, 2498–2501 (1995).
- Moss, S. C. *et al.* X-ray determination of the substrate modulation potential for a two-dimensional Rb liquid in graphite. *Phys. Rev. Lett.* **57**, 3191–3194 (1986).
- Broughton, J. Q., Bonissent, A. & Abraham, F. F. The fcc (111) and (100) crystal-melt interface: a comparison by molecular dynamics simulation. *J. Chem. Phys.* **74**, 4029–4037 (1981).
- Rhykerd, C. L., Schoen, M., Diestler, D. J. & Cushman, J. H. Epitaxy in simple classical fluids in micropores and near-solid surfaces. *Nature* **330**, 461–463 (1987).
- Curtin, W. A. Density-functional theory of the solid-liquid interface. *Phys. Rev. Lett.* **59**, 1228–1231 (1987).
- Bouchard, B. *et al.* A triple-crystal diffractometer for high-energy synchrotron radiation at the HASYLAB high-field wiggler beamline BW5. *J. Synch. Radiat.* **5**, 90–101 (1998).
- Tschentscher, Th. & Suortti, P. Experiments with very high energy synchrotron radiation. *J. Synch. Radiat.* **5**, 286–292 (1998).
- North, D. M., Enderby, J. E. & Egelstaff, P. A. The structure factor for liquid metals. *Proc. Phys. Soc. Ser. 2* **1**, 784–794; 1075–1087 (1968).
- Barton, S. W. *et al.* Distribution of atoms at the surface of liquid mercury. *Nature* **321**, 685–687 (1986).
- Grey, F., Feidenhans'l, R., Pedersen, J. S., Nielsen, M. & Johnson, R. L. Pb/Ge(111) 1x1: An anisotropic two-dimensional liquid. *Phys. Rev. B* **41**, 9519–9522 (1990).
- Dosch, H. *Critical Phenomena at Surfaces and Interfaces* (Vol. 126, Tracts in Modern Physics, Springer, Berlin, 1992).

**Acknowledgements**

We dedicate this Letter to the memory of O. Klein, who died on 23 May 2000. We thank H.R. Trebin and S.C. Moss for discussions, and H. Trenkler for assistance at the ESRF. This work was funded by the Deutsche Forschungsgemeinschaft.

Correspondence and requests for materials should be addressed to H.R. (e-mail: reichert@xray.mpi-stuttgart.mpg.de).